Inorg. Chem. **2005**, *44*, 61–72

Syntheses and Crystal Structures of Dinuclear Complexes Containing d-Block and f-Block Luminophores. Sensitization of NIR Luminescence from Yb(III), Nd(III), and Er(III) Centers by Energy Transfer from Re(I)– and Pt(II)–Bipyrimidine Metal Centers

Nail M. Shavaleev,[†] Gianluca Accorsi,[‡] Dalia Virgili,[‡] Zöe R. Bell,[†] Theodore Lazarides,[§] Giuseppe Calogero,[||] Nicola Armaroli,*[,‡] and Michael D. Ward*[,†,§]

School of Chemistry, University of Bristol, Cantock's Close, Bristol BS8 1TS, U.K., Laboratorio di Fotochimica, Istituto per la Sintesi Organica e la Fotoreattività del CNR, Via P. Gobetti 101, I-40129 Bologna, Italy, Department of Chemistry, University of Sheffield, Sheffield S3 7HF, U.K., and Istituto per i Processi Chimico Fisici del CNR, Sezione de Messina, Via La Farina 237, I-98123 Messina, Italy

Received August 16, 2004

Mononuclear complexes [Re(bpym)$(CO)_3$Cl] and [Pt(bpym)$(CC–C_6H_4CF_3)_2$] (bpym = 2,2′-bipyrimidine), in which one of the bipyrimidine sites is vacant, have been used as "complex ligands" to prepare heterodinuclear d–f complexes in which a lanthanide tris(1,3-diketonate) unit is attached to the secondary bipyrimidine site to evaluate the ability of d-block chromophores to act as antennae for causing sensitized near-infrared (NIR) luminescence from adjacent lanthanide(III) centers. The two sets of complexes so prepared are [$Re(CO)_3Cl(\mu$-bpym)Ln$(fod)_3$] (abbreviated as Re–Ln; where Ln = Yb, Nd, Er) and [$(F_3C–C_6H_4–CC)_2Pt(\mu$-bpym)Ln$(hfac)_3$] (abbreviated as Pt–Ln; where Ln = Nd, Gd). Members of both series have been structurally characterized; the metal–metal separation across the bipyrimidine bridge is ≈6.3 Å in each case. In these complexes, the ^{3}MLCT (MLCT = metal to ligand charge-transfer) luminescences of the mononuclear [Re(bpym)$(CO)_3$Cl] and [Pt(bpym)$(CC–C_6H_4CF_3)_2$] complexes are quenched by energy transfer to those lanthanides (Ln = Yb, Nd, Er) that have low-lying f–f states capable of NIR luminescence; as a result, sensitized NIR luminescence is seen from the lanthanide center following excitation of the d-block unit. In the solid state, quenching of the luminescence from the d-block chromophore is complete, indicating efficient d → f energy transfer, as a result of the short metal–metal separation across the bipyrimidine bridge. In a CH_2Cl_2 solution, partial dissociation of the dinuclear complexes into the mononuclear units occurs, with the result that some ^{3}MLCT luminescence is observed from mononuclear [Re(bpym)$(CO)_3$Cl] or [Pt(bpym)$(CC–C_6H_4CF_3)_2$] present in the equilibrium mixture. Solution UV–vis and luminescence titrations, carried out by the addition of portions of Ln$(fod)_3(H_2O)_2$ or Ln$(hfac)_3(H_2O)_2$ to the d-block complex ligands, indicate that binding of the lanthanide tris(1,3-diketonate) unit at the secondary bipyrimidine site to give the d–f dinuclear complexes occurs with an association constant of ca. 10^5 M^{-1}.

Introduction

The intense, long-lived, and line-like emission of lanthanides such as Eu(III) and Tb(III) in the visible region has made them of interest for a range of applications, from biological assays[1] to display devices,[2] and as such, their photophysical properties have received a huge amount of attention. In contrast, the longer wavelength emission of lanthanides such as Yb(III), Nd(III), Dy(III), Pr(III), and Er-

* To whom correspondence should be addressed. E-mail: m.d.ward@sheffield.ac.uk (M.D.W.); armaroli@isof.cnr.it (N.A.).
† University of Bristol.
‡ ISOF-CNR.
§ University of Sheffield.
|| IPCF-CNR.

(1) (a) Mayer, A.; Neuenhofer, S. *Angew. Chem., Int. Ed. Engl.* **1994**, *33*, 1044. (b) Faulkner, S.; Matthews, J. L. In *Comprehensive Coordination Chemistry*, 2nd ed.; Ward, M. D., Ed.; Elsevier: Oxford, U.K., 2004; Vol. 9, p 913.
(2) (a) Silver, J. In *Comprehensive Coordination Chemistry*, 2nd ed.; Ward, M. D., Ed.; Elsevier: Oxford, U.K., 2004; Vol. 9 p 689. (b) Kido, J.; Okamoto, Y. *Chem. Rev.* **2002**, *102*, 2357.

10.1021/ic048875s CCC: $30.25
Published on Web 11/20/2004

(III) in the near-infrared (NIR) region has been less well studied, although this situation is being remedied.[3] Recent interest in the photophysical properties of these lanthanide ions stems from their possible use in medical diagnostics, because the longer emission wavelengths (and hence, possibly, longer excitation wavelengths) penetrate human tissue far more effectively than does UV or visible light.[1b] In addition, NIR luminescence from metals such as Dy(III), Nd(III), and Er(III) is used as the basis for the optical amplifiers used in fiber-optic systems based on silica fibers that transmit their signals in the 1300−1550 nm region.[4]

Since lanthanide ions are very poor at absorbing light directly, because of the low extinction coefficients of the Laporte forbidden f−f transitions, energy transfer from an adjacent strongly absorbing chromophore is usually used to stimulate luminescence from lanthanides. Often, this is an aromatic ligand that strongly absorbs UV light, and being directly coordinated to the lanthanide center, it can effect fast energy transfer from the resulting ligand-based triplet state. This is the usual basis for achieving sensitized emission from Eu(III) and Tb(III).[1,2,5] However, the use of UV light to perform excitation of lanthanides with lower-energy luminescent levels is undesirable from two points of view. First, it is inefficient; the use of a 300 nm photon to stimulate 1500 nm emission from Er(III) is inelegant and wasteful of energy. Second, from the point of view of biological probes, the incident radiation must be able to penetrate the tissue sample to reach the chromophore, which rules out UV light and much of the visible spectrum.[1b] Both of these points suggest that it is desirable to design NIR-luminescent lanthanide complexes that can undergo sensitized luminescence following absorption of light at longer wavelengths. To this end, there has been a recent effort directed at attaching chromophores with relatively long wavelength absorption maxima to NIR-emissive lanthanide ions. van Veggel and co-workers have prepared complexes in which a fluorescein-based chromophore, with an absorption maximum at about 500 nm, is used to stimulate NIR luminescence from lanthanides.[6] We have demonstrated a similar behavior with lanthanide complexes of a tetrazine-based ligand having an absorption maximum at ≈500 nm.[7]

For optimum control and tunability of absorption maxima, however, having transition-metal chromophores as the energy donors offers numerous advantages. Transition-metal complexes can meet all of the following criteria: (i) a strong absorption maximum that can be selected almost anywhere in the visible or NIR region; (ii) a heavy metal ion that will facilitate intersystem crossing and give a high triplet quantum yield of the energy donor following excitation; (iii) relatively long-lived triplet excited states that will facilitate energy transfer to the adjacent lanthanide; (iv) kinetic inertness and photochemical stability; (v) in many cases, luminescence from the (unquenched) triplet state that will allow energy transfer to the lanthanide to be followed by both quenching of the donor and the appearance of sensitized emission from the lanthanide; and (vi) synthetic convenience, for example, the presence of a vacant coordination site at the periphery of the complex ("complexes-as-ligands") to which a lanthanide fragment can be attached. All of these criteria have been exploited in the field of supramolecular photochemistry of d-block metal fragments. The first examples of sensitized NIR emission from lanthanide complexes using a covalently attached d-block complex unit as the sensitizer were described only a few years ago, by the groups of van Veggel (using a $[Ru(bipy)_3]^{2+}$ or ferrocenyl unit as the energy donor)[8] and Parker (using a Pd−porphyrin unit as the energy donor).[9] More recently, Cr(III) chromophores have been used as energy donors to luminescent lanthanides in heterodinuclear helicate complexes[10] and in oxalate-bridged dinuclear complexes.[11] Other heterodinuclear assemblies incorporating a metal polypyridyl unit connected to a lanthanide, which show d−f energy transfer and subsequent NIR luminescence from the lanthanide, have been described recently by the groups of Faulkner and Coe,[12] Yanagida,[13] Pikramenou,[14] and Beer.[15]

(3) Representative recent papers describing NIR luminescence from lanthanide complexes: (a) Hebbink, G. A.; Klink, S. I.; Grave, L.; Oude Alink, P. G. B.; van Veggel, F. C. J. M. *ChemPhysChem* **2002**, *3*, 1014. (b) Faulkner, S.; Pope, S. J. A. *J. Am. Chem. Soc.* **2003**, *125*, 10526. (c) Magennis, S. W.; Ferguson, A. J.; Bryden, T.; Jones, T. S.; Beeby, A.; Samuel, I. D. W. *Synth. Met.* **2003**, *138*, 463. (d) Dickins, R. S.; Aime, S.; Batsanov, A. S.; Beeby, A.; Botta, M.; Bruce, J.; Howard, J. A. K.; Love, C. S.; Parker, D.; Peacock, R. D.; Buschmann, H. *J. Am. Chem. Soc.* **2002**, *124*, 12697. (e) Kamenskikh, I. A.; Guerrasimova, N.; Dujardin, C.; Garnier, N.; Ledoux, G.; Pedrini, C.; Kirm, M.; Petrosyan, A.; Spassky, D. *Opt. Mater. (Amsterdam)* **2003**, *24*, 267. (f) Wong, W. K.; Liang, H. Z.; Wong, W. Y.; Cai, Z. W.; Li, K. F.; Cheah, K. W. *New J. Chem.* **2002**, *26*, 275. (g) Silva, F. R. G. E.; Malta, O. L.; Reinhard, C.; Güdel, H. U.; Piguet, C.; Moser, J. E.; Bünzli, J.-C. G. *J. Phys. Chem. A* **2002**, *106*, 1670. (h) Faulkner, S.; Beeby, A.; Carrie, M. C.; Dadabhoy, A.; Kenwright, A. M.; Sammes, P. G. *Inorg. Chem. Commun.* **2001**, *4*, 187. (i) Hebbink, G. A.; Klink, S. I.; Oude Alink, P. G. B.; van Veggel, F. C. J. M. *Inorg. Chim. Acta* **2001**, *317*, 114. (j) Voloshin, A. I.; Shavaleev, N. M.; Kazakov, V. P. *J. Lumin.* **2001**, *93*, 199.

(4) (a) Tanabe, S. *C. R. Chim.* **2002**, *5*, 815. (b) Meinardi, F.; Colombi, N.; Destri, S.; Porzio, W.; Blumstengel, S.; Cerminara, M.; Tubino, R. *Synth. Met.* **2003**, *137*, 959. (c) Tanabe, S. *Glass Sci. Technol. (Frankfurt/Main)* **2001**, *74*, 67. (d) Schweizer, T.; Goutaland, R.; Martins, E.; Hewak, D. W.; Brocklesby, W. S. *J. Opt. Soc. Am. B* **2001**, *18*, 1436. (e) Hasegawa, Y.; Sogabe, K.; Wada, Y.; Yanagida, S. *J. Lumin.* **2003**, *101*, 235.

(5) Sabbatini, N.; Guardigli, M.; Lehn, J.-M. *Coord. Chem. Rev.* **1993**, *123*, 201.

(6) (a) Hebbink, G. A.; Grave, L.; Woldering, L. A.; Reinhoudt, D. N.; van Veggel, F. C. J. M. *J. Phys. Chem. A* **2003**, *107*, 2483. (b) Wolbers, M. P. O.; van Veggel, F. C. J. M.; Peters, F. G. A.; van Beelen, E. S. E.; Hofstraat, J. W.; Geurts, F. A. J.; Reinhoudt, D. N. *Chem.−Eur. J.* **1998**, *4*, 772.

(7) Shavaleev, N. M.; Pope, S. J. A.; Bell, Z. R.; Faulkner, S.; Ward, M. D. *J. Chem. Soc., Dalton Trans.* **2003**, 808.

(8) Klink, S. I.; Keizer, H.; van Veggel, F. C. J. M. *Angew. Chem., Int. Ed.* **2000**, *39*, 4319.

(9) Beeby, A.; Dickins, R. S.; FitzGerald, S.; Govenlock, L. J.; Maupin, C. L.; Parker, D.; Riehl, J. P.; Siligardi, G.; Williams, J. A. G. *Chem. Commun. (Cambridge)* **2000**, 1183.

(10) Imbert, D.; Cantuel, M.; Bünzli, J.-C. G.; Bernardinelli, G.; Piguet, C. *J. Am. Chem. Soc.* **2003**, *125*, 15698.

(11) Subhan, M. A.; Nakata, H.; Suzuki, T.; Choi, J.-H.; Kaizaki, S. *J. Lumin.* **2003**, *101*, 307.

(12) (a) Pope, S. J. A.; Coe, B. J.; Faulkner, S.; Bichenkova, E. V.; Yu, X.; Douglas, K. T. *J. Am. Chem. Soc.* **2004**, in press. (b) Pope, S. J. A.; Coe, B. J.; Faulkner, S. *Chem. Commun. (Cambridge)* **2004**, 1550.

(13) Guo, D.; Duan, C.-Y.; Lu, F.; Hasegawa, Y.; Meng, Q.-J.; Yanagida, S. *Chem. Commun. (Cambridge)* **2004**, 1486.

(14) Glover, P. B.; Ashton, P. R.; Childs, L. J.; Rodger, A.; Kercher, M.; Williams, R. M.; De Cola, L.; Pikramenou, Z. *J. Am. Chem. Soc.* **2003**, *125*, 9918.

(15) Beer, P. D.; Szemes, F.; Passaniti, P.; Maestri, M. *Inorg. Chem.* **2004**, *13*, 3965.

Chart 1

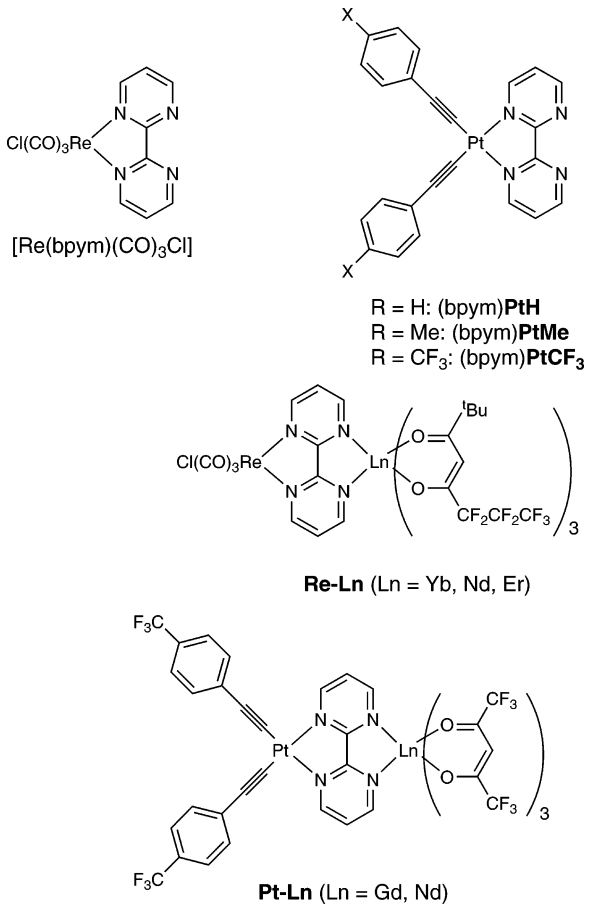

We have recently described the syntheses, structures, and photophysical properties of a series of d−f dinuclear complexes that show sensitized NIR luminescence from Yb(III), Nd(III), or Er(III) following absorption of light by the d-block chromophore in the visible region of the electromagnetic spectrum.[16−19] In many of these complexes,[16−18] a mononuclear, kinetically inert d-block complex fragment was prepared with a peripheral, vacant diimine binding site; reaction of the "complex ligand" with a lanthanide tris(diketonate) dihydrate $[Ln(dik)_3(H_2O)_2]$ (dik = diketonate) resulted in an immediate attachment of the $\{Ln(dik)_3\}$ fragment to the vacant *N*,*N*′-bidentate site of the d-block complex to give the heterodinuclear species. The syntheses are facile and high-yielding, and the method is very general, allowing a wide range of d-block chromophores and f-block luminophores to be combined.

In this paper, we describe further studies in this area based on the two series of d−f complexes shown in Chart 1, one based on a $\{Re(CO)_3Cl(diimine)\}$ unit as an energy donor and the other based on a Pt−diimine−bis(acetylide) unit as an energy donor. In both series, 2,2′-bipyrimidine is used as the bridging ligand connecting the two metal sites in order to keep the metal−metal separation short and to facilitate energy transfer. We describe the syntheses and structural characterization of the complexes and their photophysical properties, in particular, the occurrence of d → f energy transfer leading to quenching of the luminescence from the d-block unit and sensitized NIR luminescence from the lanthanide unit. Some of the synthesis (of dinuclear Re/lanthanide complexes) was outlined briefly in a preliminary communication.[16]

Results and Discussion

Preparation and Photophysical Properties of the Pt(II) Complexes. As a d-block energy-donor fragments, we investigated the known complex $[Re(bpym)(CO)_3Cl]$ (bpym = 2,2′-bipyrimidine),[20] which is weakly luminescent from its metal to ligand charge-transfer (MLCT) excited state; this would allow us to use the extent of quenching of this luminescence as a probe for studying energy transfer in the dinuclear complexes. We also investigated the new series of complexes $[Pt(bpym)(CCAr)_2]$. We were interested in using the Pt−diimine−diacetylide unit as an energy donor for two reasons. First, complexes of this type show strong luminescence from their MLCT excited states, which, as with $[Re(bpym)(CO)_3Cl]$, provides a convenient handle for studying energy transfer.[21] Second, they are synthetically convenient because the terminal diimine ligand (usually bipyridine or phenanthroline) could be replaced with bipyrimidine, therefore generating the necessary external binding site for the lanthanide unit; additionally, they are neutral and therefore soluble in the low-polarity solvents necessary to achieve optimal association of the lanthanide fragment.[21]

Reaction of $[Pt(bpym)Cl_2]$[22] with the phenylacetylene derivatives $HCC-C_6H_4X$ (X = H, Me, CF_3) in CH_2Cl_2, in the presence of $^iPr_2NH$ and a catalytic amount of CuI, afforded the complexes (bpym)PtH, (bpym)PtMe, and (bpym)$PtCF_3$ in good yield (see Chart 1 for abbreviations). Of these, (bpym)PtH and (bpym)$PtCF_3$ were structurally characterized; the molecular structures are shown in Figures 1 and 2, respectively, and selected structural parameters are collected in Tables 1 and 2. Both complexes have essentially square-planar geometry around the Pt(II), with minor distortions arising from the limited bite angle of the bipyrimidine ligand (78.9° in each case). The (unconstrained) C−Pt−C angles are 87.6° and 91.9° for (bpym)PtH and (bpym)$PtCF_3$, respectively. In both cases, the Pt−N distances (2.06−2.07 Å) are significantly longer than the Pt−C distances (1.94−1.96 Å), in agreement with related structures.[21]

The conformations of the molecules are different, however, with the molecules of (bpym)PtH being significantly distorted

(16) Shavaleev, N. M.; Bell, Z. R.; Ward, M. D. *J. Chem. Soc., Dalton Trans.* **2002**, 3925.
(17) Shavaleev, N. M.; Bell, Z. R.; Accorsi, G.; Ward, M. D. *Inorg. Chim. Acta* **2003**, *351*, 159.
(18) (a) Shavaleev, N. M.; Moorcraft, L. P.; Pope, S. J. A.; Bell, Z. R.; Faulkner, S.; Ward, M. D. *Chem.—Eur. J.* **2003**, *9*, 5283. (b) Shavaleev, N. M.; Moorcraft, L. P.; Pope, S. J. A.; Bell, Z. R.; Faulkner, S.; Ward, M. D. *Chem. Commun. (Cambridge)* **2003**, 1134.
(19) Miller, T. A.; Jeffery, J. C.; Ward, M. D.; Adams, H.; Pope, S. J. A.; Faulkner, S. *J. Chem. Soc., Dalton Trans.* **2004**, 1524.
(20) Vogler, A.; Kisslinger, J. *Inorg. Chim. Acta* **1986**, *115*, 193.
(21) (a) Whittle, E. C.; Weinstein, J. A.; George, M. W.; Schanze, K. S. *Inorg. Chem.* **2001**, *40*, 4053. (b) Hissler, M.; Connick, M.; Geiger, D. K.; McGarrah, J. E.; Lipa, D.; Lachiotte, R. J.; Eisenberg, R. *Inorg. Chem.* **2000**, *39*, 447. (c) Chan, S.-C.; Chan, M. C. W.; Wang, Y.; Che, C.-M.; Cheung, K.-K.; Zhu, N. *Chem.—Eur. J.* **2001**, *7*, 4180. (d) James, S. L.; Younus, M.; Raithby, P. R.; Lewis, J. *J. Organomet. Chem.* **1997**, *543*, 233.
(22) Kiernan, P. M.; Ludi, A. *J. Chem. Soc., Dalton Trans.* **1978**, 1127.

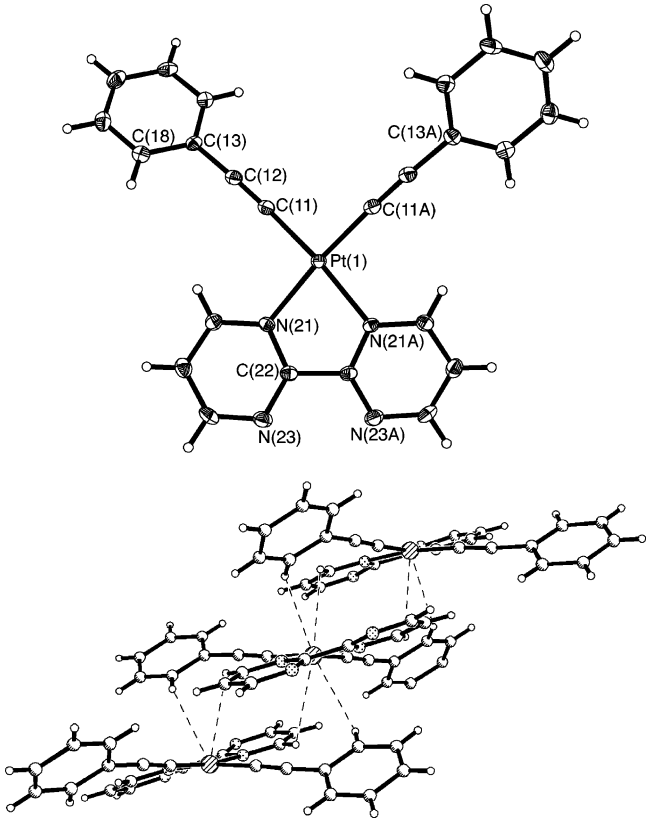

Figure 1. (a) Molecular structure of (bpym)PtH using thermal ellipsoids at the 40% probability level. (b) Packing in the crystal of (bpym)PtH.

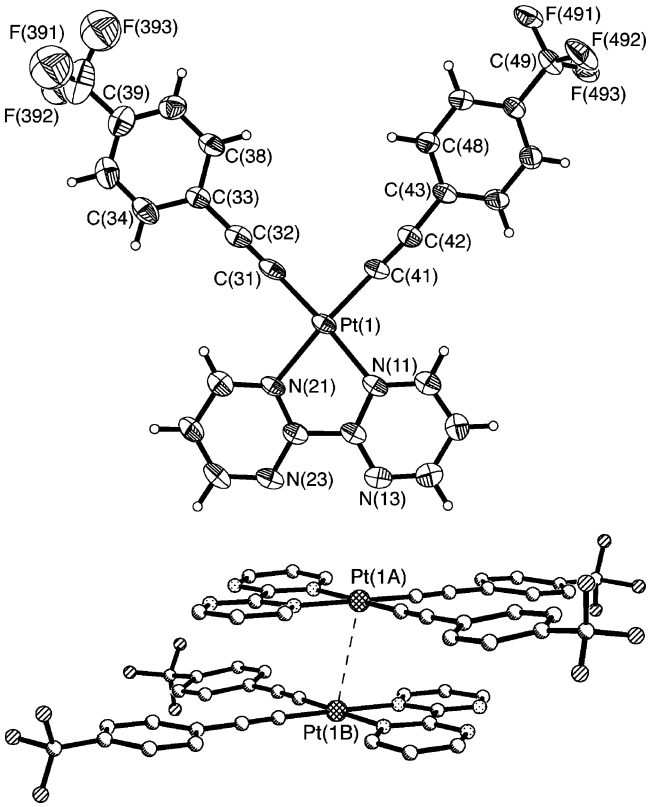

Figure 2. (a) Molecular structure of (bpym)$PtCF_3$ using thermal ellipsoids at the 40% probability level. (b) Packing in the crystal of (bpym)$PtCF_3$.

from planarity, as shown by the angle between the PtNN and PtCC planes of 11°. Thus, the molecule is "bowed",

Table 1. Selected Bond Lengths (Å) and Angles (deg) for (bpym)PtH

Pt(1)−C(11)	1.954(4)	C(11)−C(12)	1.206(5)
Pt(1)−N(21)	2.073(3)		
C(11)−Pt(1)−C(11A)	91.9(2)	C(11)−Pt(1)−N(21)	95.05(13)
C(11)−Pt(1)−N(21A)	170.14(13)	C(12)−C(11)−Pt(1)	175.2(3)
N(21A)−Pt(1)−N(21)	78.94(16)	C(22)−N(21)−Pt(1)	115.2(2)

Table 2. Selected Bond Lengths (Å) and Angles (deg) for (bpym)$PtCF_3$

Pt(1)−C(31)	1.936(8)	Pt(1)−N(21)	2.074(5)
Pt(1)−C(41)	1.956(6)	C(31)−C(32)	1.210(10)
Pt(1)−N(11)	2.060(5)	C(41)−C(42)	1.198(9)
C(31)−Pt(1)−C(41)	87.6(3)	C(12)−N(11)−Pt(1)	116.2(4)
C(31)−Pt(1)−N(11)	175.8(2)	C(16)−N(11)−Pt(1)	127.0(4)
C(41)−Pt(1)−N(11)	96.6(2)	C(26)−N(21)−Pt(1)	126.1(5)
C(31)−Pt(1)−N(21)	97.0(2)	C(22)−N(21)−Pt(1)	115.0(4)
C(41)−Pt(1)−N(21)	175.2(2)	C(32)−C(31)−Pt(1)	177.4(6)
N(11)−Pt(1)−N(21)	78.9(2)	C(42)−C(41)−Pt(1)	177.9(6)

Table 3. Photophysical Properties of the Mononuclear Complexes, Recorded in Air-Equilibrated CH_2Cl_2 at 298 K

	absorption		luminescence		
complex	λ_{max} (nm)	ϵ ($M^{-1}\,cm^{-1}$)	λ_{max} (nm)[a]	τ (ns)	$\Phi \times 10^2$
(bpym)PtMe	430[b]	7 000	612	4.8	0.01
	327	11 000			
	264[c]	62 000			
(bpym)PtH	425[b]	7 100	600	15.2	0.12
	323	11 400			
	263[c]	57 000			
(bpym)$PtCF_3$	415[b]	7 800	575	107	3.7
	269[c]	58 000			
[Re(bpym)$(CO)_3$Cl]	403[b]	2 680	689	2.1	0.011
	234[c]	24 700			

[a] Value corrected for instrumental response where necessary. [b] MLCT absorption maximum. [c] Ligand-centered absorption maximum.

with one phenyl ring lying above the mean Pt−bpym plane and the other below it. A consequence of this is the absence of well-defined columnar stacks that often arise in crystals of planar Pt(II) complexes. The closest Pt···Pt separation is 5.066 Å; the nearest interactions between each Pt center and its neighboring molecules above and below it are at H(18) and H(26), with Pt···H separations of 3.19 and 3.29 Å, respectively. In contrast, the molecules of (bpym)$PtCF_3$ are nearly coplanar, with an angle of only 1.7° between the PtNN and PtCC planes. This results in the molecules forming stacked pairs in the crystal with a pair of molecules related by an inversion center having a Pt···Pt separation of 3.392 Å (Figure 2b).

UV−vis absorption spectra and luminescence data on the mononuclear complexes are collected in Table 3. All three complexes show a MLCT transition in the 415−430 nm region, as well as more intense transitions in the UV region characteristic of ligand-centered transitions. The MLCT transitions are red-shifted compared to those of the analogous complexes with bipy or phen as the diimine ligand,[21] which is because of the lower energy of the lowest unoccupied molecular orbital of bipyrimidine arising from the two additional electronegative N atoms in the π system. Upon excitation of the MLCT transition, all three complexes show luminescence in an air-equilibrated CH_2Cl_2 solution. Like the absorption maxima, the emission maxima (between 575 and 612 nm) are also red-shifted compared to the bipy and

phen analogues; for example, emission from [(phen)Pt(CC−$C_6H_4Me)_2$] (phen = 1,20-phenanthroline) in a fluid solution occurs at 578 nm,[21] whereas (bpym)PtMe emits at 612 nm. The previously observed variations in emission intensity and lifetime that occur as the substituents on the phenyl rings are changed are clear for the bpym complexes; as these substituents become more electron-withdrawing, the absorption and emission maxima are blue-shifted and the emission quantum yield and lifetime increase. Thus, whereas (bpym)PtMe and (bpym)PtH are weakly luminescent (τ = 4.8 and 15 ns, respectively), (bpym)$PtCF_3$ has a luminescence lifetime (107 ns) and quantum yield (3.7%) comparable to $[Ru(bipy)_3]^{2+}$ (bipy = 2,2′-bipyridine) under the same conditions (Table 3). The luminescence from these complexes is less intense and shorter-lived than those previously observed from the bipy and phen analogues,[21] which may be ascribed, in part, to the energy-gap law (lower-energy luminescence tends to be weaker because of the greater likelihood of quenching by molecular vibrations); however, the previously reported measurements were performed in the absence of O_2, which will have a substantial effect, so the data are not directly comparable.

We note that aggregation of the complexes in solution is not an issue here. Planar Pt(II) complexes with diimine or related ligands are well-known to associate in the solid state (cf. some of the crystal structures described above), which has a substantial effect on their luminescence properties, with low-energy luminescence features arising either from excimers (if there is $\pi-\pi$ stacking of the aromatic ligands) or from the metal−metal-bond to ligand charge-transfer (MMLCT) excited state (if there is a Pt···Pt interaction).[23] In some cases, this association can occur in solution; however, in these cases, the photophysical properties of the complexes in solution are strongly concentration-dependent and the association requires relatively high concentrations.[24] For our mononuclear Pt(II) complexes, neither the UV−vis absorption spectra nor the steady-state luminescence spectra showed any change in their shape as samples were diluted from 10^{-4} to 10^{-6} M, spanning the concentration range that we used for photophysical studies. Also, all time-resolved measurements in solution showed only a single-exponential luminescence decay, indicating the presence of only one Pt-based emitting species.

Preparation and Structures of d−f Dinuclear Complexes. On the basis of the above results, we decided to use (bpym)$PtCF_3$ as the energy-donor component for incorporation into dinuclear complexes with lanthanides, along with $[Re(CO)_3Cl(bpym)]$. The dinuclear complexes were simply prepared by reaction of either $[Re(CO)_3Cl(bpym)]$ or (bpym)-$PtCF_3$ with the appropriate $Ln(dik)_3(H_2O)_2$ in CH_2Cl_2. Thus, equimolar amounts of $[Re(CO)_3Cl(bpym)]$ and $[Yb(fod)_3(H_2O)_2]$ (fod = $^tBuC(O)CH_2C(O)CF_2CF_2CF_3$; see Chart 1) in CH_2Cl_2 were combined, giving an immediate darkening of the color of the Re chromophore; the addition of hexane, followed by slow evaporation, afforded crystals of $[Re(CO)_3Cl(\mu$-bpym)Yb$(fod)_3]$ (Re−Yb**)** in good yield. The analogous complexes Re−Nd and Re−Er were obtained in the same way. Similarly, equimolar amounts of (bpym)$PtCF_3$ and $[Nd(hfac)_3(H_2O)_2]$ (hfac = $CF_3C(O)CH_2C(O)CF_3$; see Chart 1) dissolved in benzene were combined, giving an immediate color change of the Pt chromophore from orange to red as the dinuclear complex formed; the addition of heptane, followed by slow evaporation of the solvent, afforded a good crop of crystals of $[(F_3C-C_6H_4-CC)_2Pt(\mu$-bpym)Nd$(hfac)_3]$ (Pt−Nd); the complex Pt−Gd was prepared in the same way. The complexes are air stable and were characterized on the basis of correct elemental analyses. Mass spectrometry was unhelpful, showing only peaks for the mononuclear metal species and their fragments. Several of the complexes were also characterized by X-ray crystallography.

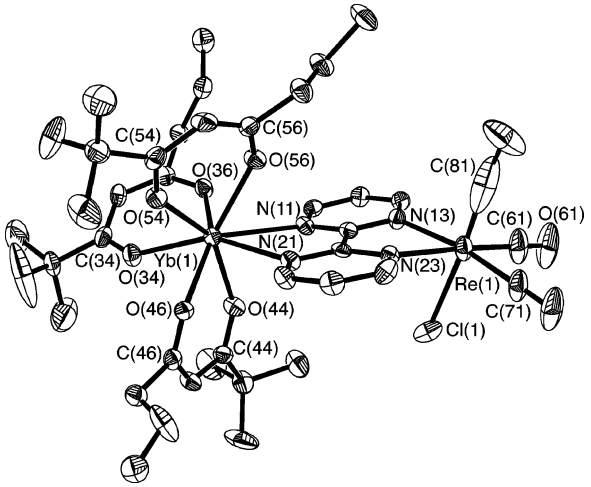

Figure 3. Molecular structure of Re−Yb using thermal ellipsoids at the 40% probability level (F atoms from the "fod" ligands are omitted for clarity). The elongated thermal ellipsoid of C(81) reflects slight, unresolved disorder of that CO ligand with the trans ligand Cl(1).

The molecular structure of Re−Er was described in the recent preliminary communication and is not reproduced here.[16] The structure of Re−Yb is very similar and is shown in Figure 3; selected bond lengths and angles are in Table 4. The Re center has its usual *fac*-octahedral geometry with unremarkable bond distances and angles.[17,25] The Yb center is in a distorted-square antiprismatic eight-coordinate geometry, characteristic of $[Ln(dik)_3(diimine)]$ species.[17,18] The atoms comprising the approximate square planes are N(11)/N(21)/O(46)/O(44) (average deviation of these from the mean plane through them: 0.286 Å) and O(54)/O(56)/O(36)/O(34) (average deviation of these from the mean plane through them: 0.238 Å); these mean planes are nearly coplanar, with an angle of 2.4° between them. The Re···Yb distance is 6.23 Å; the bridging bipyrimidine ligand is near-planar.

(23) (a) Houlding, V. H.; Miskowski, V. M. *Coord. Chem. Rev.* **1991**, *111*, 145. (b) Kato, M.; Kosuge, C.; Morii, K.; Ahn, J. S.; Kitagawa, H.; Mitani, T.; Matsushita, M.; Kato, T.; Yano, S.; Kimura, M. *Inorg. Chem.* **1999**, *38*, 1638. (c) Connick, W. B.; Henling, L. M.; Marsh, R. E.; Gray, H. B. *Inorg. Chem.* **1996**, *35*, 6261.

(24) (a) Arena, G.; Calogero, G.; Campagna, S.; Scolaro, L. M.; Ricevuto, V.; Romeo, R. *Inorg. Chem.* **1998**, *37*, 2763. (b) Bailey, J. A.; Hill, M. G.; Marsh, R. E.; Miskowski, V. M.; Schaefer, W. P.; Gray, H. B. *Inorg. Chem.* **1995**, *34*, 4591.

(25) Shavaleev, N. M.; Barbieri, A.; Bell, Z. R.; Ward, M. D.; Barigelletti, F. *New J. Chem.* **2004**, *28*, 398.

Table 4. Selected Bond Lengths (Å) and Angles (deg) for Re−Yb

Yb(1)−O(36)	2.223(6)	Re(1)−C(81)	1.74(3)
Yb(1)−O(54)	2.235(6)	Re(1)−C(71)	1.925(12)
Yb(1)−O(44)	2.240(6)	Re(1)−C(61)	1.931(13)
Yb(1)−O(34)	2.269(7)	Re(1)−N(23)	2.172(8)
Yb(1)−O(46)	2.284(6)	Re(1)−N(13)	2.187(8)
Yb(1)−O(56)	2.298(7)	Re(1)−Cl(1)	2.465(3)
Yb(1)−N(21)	2.517(7)		
Yb(1)−N(11)	2.568(7)		
C(81)−Re(1)−C(71)	88.8(6)	C(61)−Re(1)−N(13)	98.9(4)
C(81)−Re(1)−C(61)	92.2(7)	N(23)−Re(1)−N(13)	74.5(3)
C(71)−Re(1)−C(61)	87.5(5)	C(81)−Re(1)−Cl(1)	175.5(5)
C(81)−Re(1)−N(23)	94.3(5)	C(71)−Re(1)−Cl(1)	94.8(4)
C(71)−Re(1)−N(23)	98.3(4)	C(61)−Re(1)−Cl(1)	90.7(5)
C(61)−Re(1)−N(23)	171.3(4)	N(23)−Re(1)−Cl(1)	82.5(2)
C(81)−Re(1)−N(13)	97.6(5)	N(13)−Re(1)−Cl(1)	78.5(2)
C(71)−Re(1)−N(13)	170.6(4)		

The molecular structures of Pt−Gd and Pt−Nd are shown in Figures 4 and 5; selected bond lengths and angles are in Tables 5 and 6. The structures are very similar to each other. The coordination environment around the Pt center is not substantially perturbed by attachment of the lanthanide unit at the secondary site; in particular, the Pt−N bond distances are not significantly different from their values in the mononuclear unit (bpym)$PtCF_3$. The lanthanide centers, however, are now nine-coordinate, with a water molecule coordinated in addition to the four bidentate chelating ligands. This is unusual because the crystal structures of $Ln(dik)_3$(diimine) complexes, including many that we have structurally characterized,[16−18] are eight-coordinate; the presence of the ninth ligand in these crystal structures is presumably a kinetic effect, arising from the favorable crystallization of

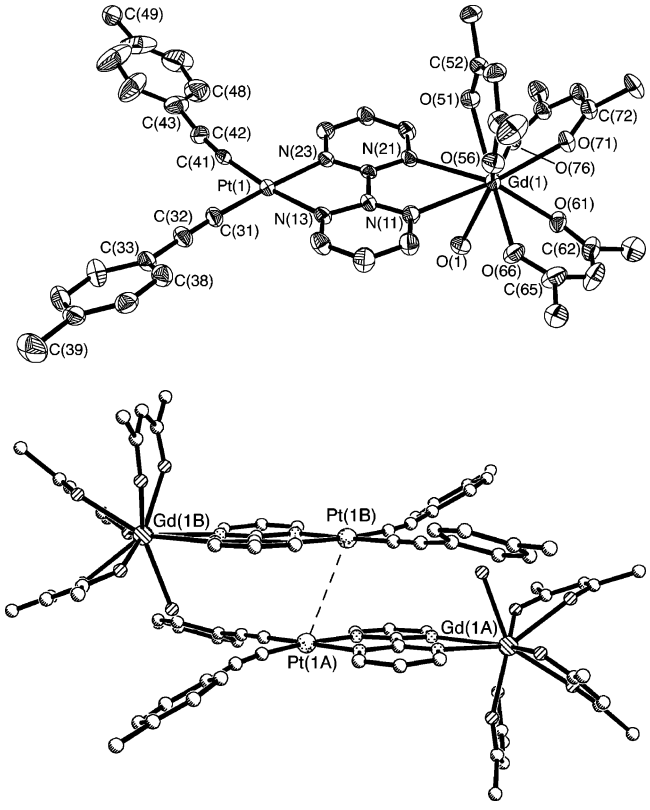

Figure 4. (a) Molecular structure of Pt−Gd using thermal ellipsoids at the 40% probability level (F atoms are omitted for clarity). (b) Packing in the crystal of Pt−Gd.

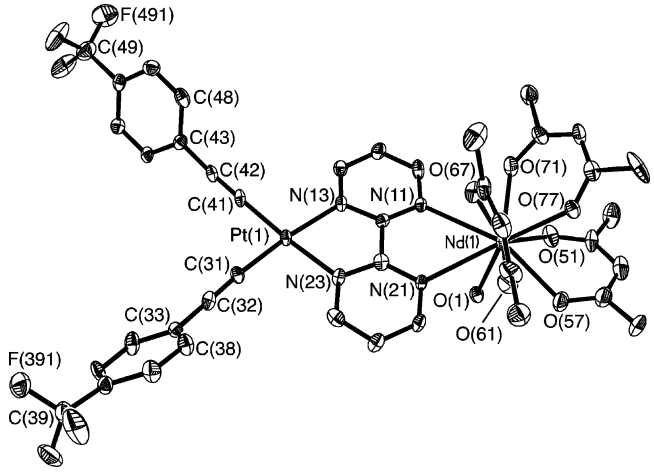

Figure 5. Molecular structure of one of the two crystallographically independent molecules of Pt−Nd using thermal ellipsoids at the 40% probability level (F atoms from the "hfac" ligands are omitted for clarity).

Table 5. Selected Bond Lengths (Å) and Angles (deg) for Pt−Gd·(C_6H_6)

Gd(1)−O(66)	2.338(6)	Gd(1)−N(11)	2.660(6)
Gd(1)−O(71)	2.351(5)	Gd(1)−N(21)	2.680(6)
Gd(1)−O(76)	2.375(5)	Pt(1)−C(41)	1.932(9)
Gd(1)−O(56)	2.388(6)	Pt(1)−C(31)	1.944(8)
Gd(1)−O(51)	2.397(6)	Pt(1)−N(13)	2.067(7)
Gd(1)−O(61)	2.412(5)	Pt(1)−N(23)	2.069(6)
Gd(1)−O(1)	2.475(6)		
C(41)−Pt(1)−C(31)	91.7(3)	C(41)−Pt(1)−N(23)	94.6(3)
C(41)−Pt(1)−N(13)	173.1(3)	C(31)−Pt(1)−N(23)	173.3(3)
C(31)−Pt(1)−N(13)	94.4(3)	N(13)−Pt(1)−N(23)	79.2(2)

Table 6. Selected Bond Lengths (Å) and Angles (deg) for Pt−Nd·(C_6H_6)

Nd(1)−O(71)	2.367(7)	Nd(2)−O(167)	2.404(6)
Nd(1)−O(61)	2.420(7)	Nd(2)−O(171)	2.426(6)
Nd(1)−O(77)	2.421(6)	Nd(2)−O(177)	2.428(6)
Nd(1)−O(57)	2.425(7)	Nd(2)−O(161)	2.432(6)
Nd(1)−O(67)	2.442(6)	Nd(2)−O(151)	2.432(6)
Nd(1)−O(51)	2.476(7)	Nd(2)−O(157)	2.484(6)
Nd(1)−O(1)	2.507(6)	Nd(2)−O(2)	2.534(6)
Nd(1)−N(21)	2.712(7)	Nd(2)−N(111)	2.683(7)
Nd(1)−N(11)	2.787(7)	Nd(2)−N(121)	2.708(7)
Pt(1)−C(31)	1.937(9)	Pt(2)−C(131)	1.943(8)
Pt(1)−C(41)	1.947(9)	Pt(2)−C(141)	1.945(8)
Pt(1)−N(23)	2.052(7)	Pt(2)−N(113)	2.061(7)
Pt(1)−N(13)	2.073(7)	Pt(2)−N(123)	2.075(7)
C(31)−Pt(1)−C(41)	89.1(4)	C(131)−Pt(2)−C(141)	90.1(4)
C(31)−Pt(1)−N(23)	94.2(3)	C(131)−Pt(2)−N(113)	95.7(3)
C(41)−Pt(1)−N(23)	176.3(3)	C(141)−Pt(2)−N(113)	173.5(3)
C(31)−Pt(1)−N(13)	173.3(3)	C(131)−Pt(2)−N(123)	174.3(3)
C(41)−Pt(1)−N(13)	97.5(3)	C(141)−Pt(2)−N(123)	94.3(3)
N(23)−Pt(1)−N(13)	79.3(3)	N(113)−Pt(2)−N(123)	79.7(3)

this particular form, even if it is not the dominant structure in solution. The Pt···Gd distance across the planar bipyrimidine ligand is 6.263 Å. As we saw for (bpym)$PtCF_3$, the planar Pt fragments (angle between the PtNN and PtCC planes: 3.6°) stack across an inversion center, giving an axial Pt···Pt contact of 3.497 Å between adjacent molecules in a stacked pair. Pt−Nd has a very similar molecular structure but a different crystal structure with two independent complex molecules in the asymmetric unit. As with Pt−Gd, each molecule of Pt−Nd stacks with its symmetry equivalent across an inversion center; the Pt(1)···Pt(1′) separation is 3.758 Å, and the Pt(2)···Pt(2′) separation is 3.348 Å. Within

the two independent molecules, the Pt···Nd separations are 6.335 and 6.286 Å.

Solution Behavior of the Dinuclear Complexes: UV−Vis Spectra, Steady-State Luminescence, and Association Constants. Binding of a $[Ln(dik)_3(H_2O)_2]$ unit to diimines (NN), according to eq 1, to give the eight-coordinate diimine adduct with liberation of two molecules of water is known to be a reversible process, with equilibrium constants of up to $\approx 10^7$ M^{-1} for NN = 2,2′-bipyridine or 1,10-phenanthroline in hydrocarbon solvents.[26]

$$[Ln(dik)_3(H_2O)_2] + NN = [Ln(dik)_3(NN)] + 2H_2O \quad (1)$$

With less-basic NN ligands, the equilibrium constant is correspondingly reduced. For example, we recently observed binding constants on the order of 10^4 M^{-1} in CH_2Cl_2 for the association of $[Ln(dik)_3(H_2O)_2]$ to the vacant NN site of complexes such as $[Cl_2Pt(dppz)]$ [dppz = 2,3-di(2-pyridyl)-pyrazine] in which one of the vacant N donors is a pyrazine rather than a pyridine ring.[18a] The result is that, at the concentrations typically used for luminescence and UV−vis spectroscopic studies, partial dissociation of the dinuclear d−f complexes occurs, which complicates the luminescence analysis in solution. Given the relatively low basicity of pyrimidine compared to that of pyridine (pK_a values in water of 1.3 and 5.2, respectively), it was felt that this was likely to be an issue with these complexes, and accordingly, UV−vis and luminescence titrations on representative systems were carried out. A representative example is shown in Figure 6.

The addition of portions of $[Ln(hfac)_3(H_2O)_2]$ (Ln = Gd, Yb) to a solution of $(bpym)PtCF_3$ in dry CH_2Cl_2 resulted in a deepening of the orange color of the Pt chromophore, which is associated with the MLCT transition being reduced in energy and shifted more into the visible region, from 415 to 425 nm (Figure 6a). A graph of absorbance at a selected wavelength versus the amount of $[Ln(hfac)_3(H_2O)_2]$ added gave a smooth curve that fitted well to a 1:1 binding isotherm (Figure 6c), from which the association constant for binding of the lanthanide fragment to the diimine site (equilibrium constant for eq 1) could be determined; the values obtained were 3.5 (±0.3) × 10^5 M^{-1} for Pt−Yb and 1.2 (±0.2) × 10^5 M^{-1} for Pt−Gd. These are rather low compared to the values obtained for other lanthanide−diimine adducts with ligands such as bipyridine and phenanthroline,[26] and they are low as a consequence of the poor basicity of bipyrimidine. The slightly higher K_a value for Pt−Yb compared to that of Pt−Gd presumably reflects the smaller ionic radius and higher charge density of Yb(III). It is not appropriate to overanalyze these binding constants because we found that they are very sensitive to traces of moisture in the solvent; the use of ordinary undried CH_2Cl_2 from a fresh bottle afforded binding constants 2 orders of magnitude lower. The important point is that, with K_a values of ca. 10^5 M^{-1}, significant dissociation is to be expected at the concentrations typically used for luminescence measurements in solution ($\approx 10^{-5}$ M).

(26) Yajima, S.; Hasegawa, Y. *Bull. Chem. Soc. Jpn.* **1998**, *71*, 2825.

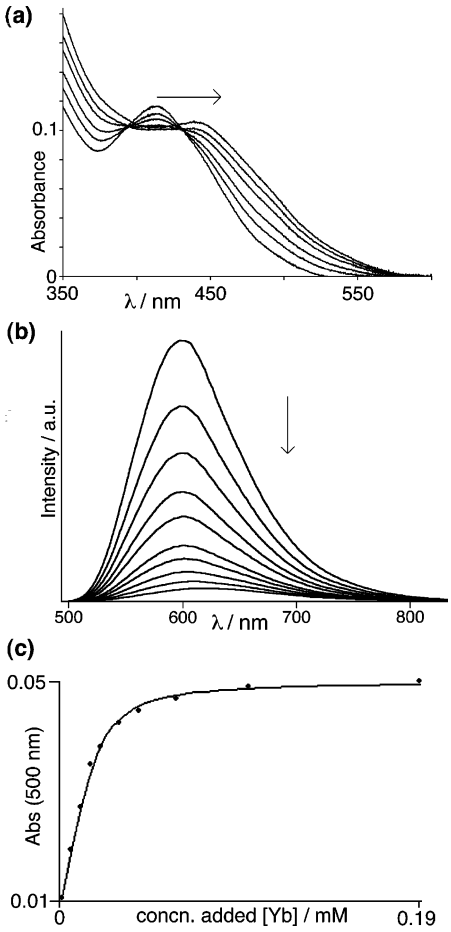

Figure 6. Titration of $(bpym)PtCF_3$ with $Yb(hfac)_3(H_2O)_2$ in a CH_2Cl_2 solution: (a) red shift in the MLCT absorption maximum of $(bpym)PtCF_3$; (b) quenching of Pt-based luminescence; (c) absorbance values at 500 nm during titration (dots) fitted to a 1:1 binding isotherm (line) to give K_a = 3.5 × 10^5 M^{-1}.

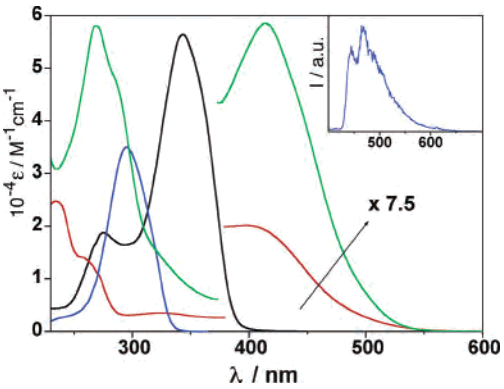

Figure 7. Electronic absorption spectra of $[Re(bpym)(CO)_3Cl]$ (red), $(bpym)PtCF_3$ (green), $[Nd(tta)_3(H_2O)_2]$ (black), and $[Yb/Er(fod)_3(H_2O)_2]$ (blue). Above 400 nm, the spectra are multiplied by a factor of 7.5. Inset: phosphorescence spectra of $[Gd(fod)_3(H_2O)_2]$ at 77 K in CH_2Cl_2, λ_{exc} = 294 nm.

Luminescence spectra were also recorded during the titrations. With Ln = Yb, binding of the lanthanide fragment results in complete quenching of the luminescence of free $(bpym)PtCF_3$ (Figure 6b). In contrast, when Ln = Gd, there is some quenching of the $(bpym)PtCF_3$ luminescence, but this is not complete, and about 15% of the original luminescence intensity remains after the addition of excess $[Gd(hfac)_3(H_2O)_2]$. This implies two things. First, binding

of a lanthanide fragment to the secondary site of (bpym)-$PtCF_3$ provides an additional pathway for quenching of the Pt-based luminescence, either by providing additional vibrational pathways for deactivation of the excited state or by perturbation of the ^{3}MLCT level that is due to the presence of a +3 charge. These effects alone do not result in complete quenching, as shown by the Pt−Gd system, where there is residual luminescence; it is important to note that Gd(III) cannot act as an energy acceptor because its first electronically excited state is far too high in energy (≈32 000 cm^{-1}). In contrast, in the Pt−Yb system, quenching is complete because of the ability of Yb(III) to act as an energy acceptor through its low-lying $^2F_{5/2}$ level. The presence of incomplete quenching of the Pt-based luminescence when Ln = Gd but complete quenching when Ln = Yb indicates that Pt → Yb photoinduced energy transfer is taking place in the latter case and we should see sensitized luminescence from Yb(III) following excitation of the (bpym)$PtCF_3$ center.

A similar titration experiment was performed on the [Re-(bpym)$(CO)_3$Cl]/ Yb$(fod)_3$ system with similar results. Binding of the Yb$(fod)_3$ fragment at the vacant diimine site results in a red shift of the MLCT absorption in the UV−vis spectrum, from 403 nm to a shoulder at ca. 440 nm. From the changes in the spectral data, an association constant for lanthanide binding in Re−Yb of 1.9 (±0.2) × 10^5 M^{-1} cm^{-1} was determined, comparable to the values obtained for the Pt−Ln complexes.

Photophysical Properties of the Dinuclear Complexes. Photophysical properties of dinuclear Re−Ln (Ln = Nd, Yb, and Er) and Pt−Nd complexes were investigated in a CH_2Cl_2 solution. For the sake of comparison, mononuclear compounds [Re(bpym)$(CO)_3$Cl], (bpym)$PtCF_3$, [Nd$(tta)_3(H_2O)_2$] (tta = 2-thenoyltrifluoroacetone), [Yb$(fod)_3(H_2O)_2$], and [Er$(fod)_3(H_2O)_2$] have also been studied; the absorption spectra are depicted in Figure 7. For the Nd(III) complexes, the light-absorbing antenna unit is the diketonate ligand tta or hfac; for Yb(III) and Er(III) analogues, this role is played by fod. The presence of different ligands is reflected in the different UV absorption profiles.

As mentioned above, the lowest electronic excited states of [Re(bpym)$(CO)_3$Cl][20,27] and (bpym)$PtCF_3$[21] are of a ^{3}MLCT nature, and they are located at 2.19 eV for the former[20] and 2.39 eV for the latter (determined from the emission maximum of 518 nm in a frozen MeOH/EtOH glass). For the mononuclear lanthanide complexes, UV excitation of the ligand-centered bands results in typical luminescence of the corresponding Ln(III) ion in the NIR spectral region, with energy levels below 1.4 eV. This is a consequence of an energy-transfer process from the diketonate ligand to the corresponding metal ion. The sensitization process in lanthanide complexes occurs from the ligand triplet levels[5] that, for fod/hfa and tta, are positioned at 2.80 and 2.57 eV, respectively, according to the phosphorescence spectra of the reference Gd(III) complexes[5] (see, for example, the inset of Figure 8).

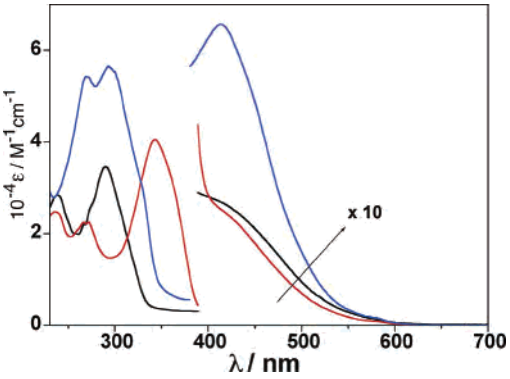

Figure 8. Electronic absorption spectra of Re−Yb/Er (black), Re−Nd (red), and Pt−Nd (blue) in a CH_2Cl_2 solution. Above 400 nm, the spectra are multiplied by a factor of 10. The dinuclear complexes undergo partial dissociation; therefore, the spectra reflect a mixture of dissociated and undissociated samples (see text).

From this energy level description, the dinuclear complexes Re−Ln and Pt−Ln possess an energy gradient allowing energy transfer from the d-block to the f-block moiety. The absorption spectra of Re−Ln and Pt−Nd in a CH_2Cl_2 solution are depicted in Figure 8. The UV spectral range is characterized by ligand-centered transitions. The contribution of the bpym chelating ligand is of minor importance and only observable in the peak/shoulders around 235 nm (see the spectrum of [Re(bpym)$(CO)_3$Cl] in Figure 7). The remarkable differences observed in the various cases are related to the presence of the three different diketonate ligands (fod, tta, and hfa) that exhibit distinct UV absorption profiles (Figure 7); these are the origin of the absorption between 300 and 400 nm. For dinuclear complexes, by inspecting the absorption spectra of mononuclear compounds in Figure 8, one can assign the absorption features at wavelengths longer than 400 nm to MLCT transitions of the Re- or Pt-complexed moiety. The intensity of the Pt(II) ← bpym MLCT absorption band is substantially stronger than that of the Re(I) ← bpym absorption. Of course, in these conditions, there will be some dissociation of the dinuclear complex (eq 1), but the main features of the complexes [viz., the diketonate-centered transitions at 300−400 nm and the MLCT transition of the d-block fragment at λ > 400 nm] are only slightly affected by this, and apart from the shift in the MLCT absorption of the d-block unit in the dinuclear complexes, the spectra of the dinuclear complexes are approximately the sum of the spectra of the two chromophores.

Upon excitation of the MLCT band of the Re moiety at 460 nm, all of the dinuclear Re−Ln complexes exhibit the NIR emission features of the lanthanide ion (Figure 9). Because no direct excitation of the lanthanide moiety occurs at this wavelength, the observed NIR emission signals can only arise by sensitization of the lanthanide ions from the Re-complexed moiety, following energy transfer.[8,12−15,19] As expected, three emission bands were observed for Nd(III) at 866, 1060, and 1330 nm ($^4I_{9/2}$, $^4I_{11/2}$, $^4I_{13/2}$ ← $^4F_{3/2}$, respectively), one for Yb(III) at 975 nm ($^2F_{7/2}$ ← $^2F_{5/2}$), and one for Er(III) at 1535 nm ($^4I_{15/2}$ ← $^4I_{13/2}$) (Figure 10).[28] Following the measurements of association constants described above, it is to be expected that partial dissociation

(27) Armaroli, N.; Accorsi, G.; Felder, D.; Nierengarten, J. F. *Chem.—Eur. J.* **2002**, *8*, 2314.

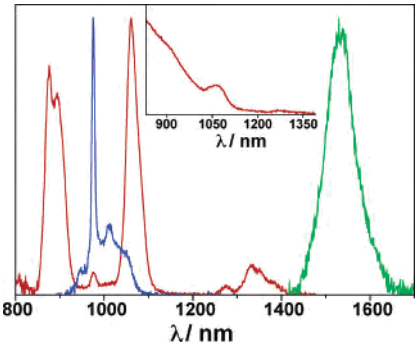

Figure 9. Corrected and normalized emission spectra from Re−Nd (red), Re−Yb (blue), Re−Er (green), and Pt−Nd (red, inset) in CH_2Cl_2 solutions, λ_{exc} = 460 nm, absorbance at excitation wavelength = 0.2.

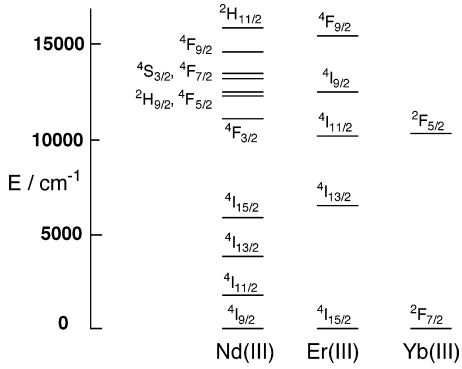

Figure 10. Approximate energy levels for Nd(III), Er(III), and Yb(III).

of the Re−Ln complexes into their mononuclear complexes will occur (eq 1). Indeed, weak ^{3}MLCT luminescence from [Re(bpym)$(CO)_3$Cl] was observed, with a quantum yield corresponding to about 20% dissociation of the dinuclear Re−Ln complexes. The lifetime of this excited state (2.1 ns) is the same as that of free [Re(bpym)$(CO)_3$Cl]. No shorter-lived ^{3}MLCT luminescence component was detected, indicating that, in the intact Re−Ln complexes, the Re-based luminescence is completely quenched (or is reduced to a subnanosecond lifetime) because of fast Re → Ln energy transfer (Ln = Yb, Nd, Er). The quenching is therefore stronger than that observed in some other dinuclear lanthanide complexes with $[Ru(bpy)_n]^{2+}$-type moieties as energy donors, where residual ^{3}MLCT luminescence from the d-block unit is observed.[8,12,13,15,19] In the present case, the close proximity of the two metal centers allows a very fast energy transfer, which can compete successfully with the fast intrinsic ^{3}MLCT deactivation. Fortunately, the weakness of the residual ^{3}MLCT luminescence from free [Re(bpym)$(CO)_3$Cl] means that its low-energy tail does not significantly interfere with the lanthanide luminescence measurements of the Re−Ln series in the NIR region (Figure 9).

To test whether any change of the emission yield of the Ln moiety occurs in the dinuclear complexes, we compared the emission yields of the Re−Ln compounds with that of the corresponding mononuclear lanthanide complex upon excitation in the UV region. A small increase of the NIR emission intensity in Re−Nd and Re−Yb was detected when

Table 7. Lanthanide Emission Properties for the Dinuclear Complexes in Solution and in the Solid State at 298 K

	CH_2Cl_2		solid state		
	λ_{max} (nm)[a]	τ (μs)[b]	λ_{max} (nm)[a]	$\Phi_{em} \times 10^{-4}$ [c]	τ (μs)[b]
Re−Yb	975	6.7	975	79	9.6
	975[d]		975[d]		
Re−Er	1534	<0.5	1534	2	1.6
	1538[d]		1538[d]		
Re−Nd	1061	<0.5	1061	24	0.9
	1061[d]	0.44[e]	1061[d]		
Pt−Nd	1061	<0.5	1061	27	1.0
	1061[d]		1061[d]		

[a] λ_{exc} = 460 nm. [b] λ_{exc} = 355 nm, laser excitation. [c] Φ_{em} for metal-based luminescence only, calculated from eq 2 (see the main text). [d] Corrected values for instrumental response. [e] Measured with a UV−vis detector at λ_{em} = 880 nm.

compared to the intensity detected in mononuclear species [Nd(tta)$_3$$(H_2O)_2$] and [Yb(fod)$_3$$(H_2O)_2$] (in the case of Re−Er, the emission is so weak that quantitative considerations are prevented). This is probably related to the replacement of solvent molecules by *N*,*N*′-bipyrimidine in the Ln(III) coordination sphere, which could depress nonradiative deactivation pathways through vibrational quenching, as we have seen before when comparing [Ln(dik)$_3$$(H_2O)_2$] and [Ln(dik)$_3$(diimine)] luminophores.[29]

Excitation of Pt−Nd into the MLCT Pt-based band (460 nm) in CH_2Cl_2 also gives rise to Nd(III) emission in the NIR region, confirming that Pt → Nd energy transfer occurs. However, in this case, an intense MLCT emission band at λ_{max} = 575 nm is also observed, and the band's low-energy tail partially overlaps the sharp emission features of the Nd(III) center (inset of Figure 9). As mentioned above, residual ^{3}MLCT luminescence has been observed in many cases in dinuclear d−f complexes with Ru(II)−polypyridine-type sensitizing units, and on the basis of lifetime measurements, this has been related to a slow Ru → Ln energy-transfer process that undergoes competition from intrinsic deactivation of the ^{3}MLCT level of the Ru-complexed moiety.[8,12,13,15,19] However, upon excitation at 460 nm, we find identical ^{3}MLCT lifetimes for (bpym)$PtCF_3$ and Pt−Nd (107 ns), indicating that, for the latter, we are seeing luminescence from free (bpym)$PtCF_3$ as a result of partial dissociation of the complex into its mononuclear components. For intact Pt−Nd, the Pt-based luminescence should be completely quenched, as shown by the titration measurements (above) and by the solid-state luminescence data (below). The inherently strong luminescence of free (bpym)$PtCF_3$ accounts for the sensitized NIR luminescence from Nd(III) being partially obscured by the tail of the ^{3}MLCT luminescence.

To avoid the dissociation process and get "clean" luminescence data in the NIR region, we also measured emission spectra (λ_{exc} = 460 nm) and lifetimes of the dinuclear complexes in the solid state as powders; data are reported in Table 7. In the solid state, no residual MLCT emission is observed for any complex, of either Re or Pt type, confirming that, in the intact dinuclear complexes, the energy-transfer process from the d-block to the f-block metal centers is very

(28) Werts, M. H. V.; Hofstraat, J. W.; Geurts, F. A. J.; Verhoeven, J. W. *Chem. Phys. Lett.* **1997**, *276*, 196.

(29) Shavaleev, N. M.; Pope, S. J. A.; Bell, Z. R.; Faulkner, S.; Ward, M. D. *J. Chem. Soc., Dalton Trans.* **2003**, 808.

efficient. On the basis of eq 2, taking the measured values of solid samples (τ_{obs}) and the radiative ("natural") lifetimes of Nd(III), Yb(III), and Er(III) ions (τ_R) as reported in the literature,[30] we obtain emission quantum yield values of the lanthanide ion for dinuclear compounds. Such values are comparable to those previously reported for NIR-emitting Ln(III) complexes in the solid state.[27]

$$\Phi_{em} = \tau_{obs}/\tau_R \quad (2)$$

Discussion of Possible Energy-Transfer Mechanisms. The mechanisms operative for d → f energy-transfer processes are not clearly known. The energy transfer is principally determined by the distance between energy-donor and lanthanide units, as well as by the normalized overlap between the emission spectrum of the donor and the absorption spectrum of the lanthanide ion.[31,32] The acceptor level(s) on the lanthanide should be sufficiently below the ^{3}MLCT level of the donor to provide a good driving force for energy transfer and prevent back energy transfer[33] but not so much as to prevent good spectral overlap. In addition, there are separate selection rules for Förster and Dexter energy transfer, with the former requiring $|\Delta J| = 2$, 4, or 6 at the lanthanide and the latter requiring $|\Delta J| = 0$ or 1 (with the exception of $J = J' = 0$, which is forbidden).[34] It is also known that Dexter energy transfer also requires electronic coupling (orbital overlap) between energy-donor and -acceptor components,[31] whereas Förster energy transfer does not.[32] In the complexes described here, the emission spectrum of the donor unit in the dinuclear complexes is not exactly known because the donor luminescence is quenched, but we can take the emission spectra of the mononuclear Pt and Re complexes as guides. Taking their emission maxima and allowing 1000−2000 cm^{-1} as a minimum gradient for energy transfer, we need to consider energy-acceptor levels of up to ca. 16 000 cm^{-1} for Pt−Nd and slightly less for the Re−Ln diads.

In Pt−Nd, there are seven closely spaced energy levels on Nd(III) between ca. 11 000 and 16 000 cm^{-1} (Figure 10) that will overlap with the low-energy side of the broad ^{3}MLCT luminescence from the Pt unit; for Re−Nd, the highest of these is probably not relevant. If the Pt chromophores in Pt−Nd have additional MMLCT or excimer $\pi-\pi^*$ levels in the solid state arising from the crystal packing (which would be lower than the ^{3}MLCT state in energy; see Figure 4b),[23] then these would provide additional spectral overlap with the Nd(III) f−f levels. The ground state of Nd(III) is $^4I_{9/2}$, which means that the $^2H_{11/2}$, $^4F_{9/2}$, $^4F_{7/2}$, and $^2H_{9/2}$ levels could be populated by Dexter energy transfer ($|\Delta J| = 1$, 0, 1, and 0, respectively, from the ground state) and the $^4F_{5/2}$ level could be populated by Förster energy transfer ($|\Delta J| = 2$ with respect to the ground state). Energy transfer to the $^4F_{3/2}$ and $^4S_{3/2}$ levels is theoretically forbidden because $|\Delta J| = 3$. The short metal−metal distance and the conjugated bridging ligand, which will provide an orbital coupling pathway, mean that both Förster and Dexter energy-transfer mechanisms are perfectly feasible; together with the large number of possible energy-acceptor levels on Nd(III), it is not surprising that the Pt-diimine ^{3}MLCT donor state is completely quenched by Nd(III).

For Er(III), the ground state is $^4I_{15/2}$. Energy transfer to $^4I_{13/2}$ at 6500 cm^{-1}, although allowed by the Dexter mechanism, can be ruled out because of the large difference in energy between donor and acceptor states, which would give a very poor spectral overlap and make the process slow. Energy transfer to $^4I_{11/2}$ at 10 000 cm^{-1} is, however, Förster-allowed ($|\Delta J| = 2$). The only other two states that have appropriate energies are $^4I_{9/2}$ and $^4F_{9/2}$ (Figure 10), which have $|\Delta J| = 3$, and energy transfer to these is not allowed by either the Förster or Dexter mechanism. This leaves the $^4I_{11/2}$ level, which will overlap poorly with the weak tail end of the ^{3}MLCT donor emission spectrum, as the sole energy acceptor. It is, on the face of it, surprising that the d → f energy transfer in Re−Er is fast; of course, it may be much slower than that in Re−Nd and Pt−Nd, where energy transfer is more favorable, but it is still faster than our equipment can resolve (300 ns).

A similar argument applies to Re−Yb, for which there is also only a single acceptor level: energy transfer to $^4F_{5/2}$, lying at 10 200 cm^{-1}, is Dexter-allowed ($|\Delta J| = 1$ with respect to the ground state). As with Re−Er, this acceptor level will overlap only poorly with the long-wavelength tail of the ^{3}MLCT donor, and such a situation in other d−f systems containing Yb(III) as an energy acceptor is known to result in incomplete energy transfer.[8,19] Yet, the Re-based luminescence in Re−Yb is completely quenched, and the rise time for Yb(III) luminescence is faster than our instrument could detect. The combination of short metal−metal separation and strong electronic coupling provided by the bridging ligand may counteract the other limitations to energy transfer in this system.

Thus, energy transfer in these complexes could plausibly occur by either Förster or Dexter mechanisms, or [for Nd(III)] both. The occurrence of Dexter energy transfer has been recently demonstrated for sensitized Sm(III) luminescence by Bünzli and co-workers.[35] Contrarily, the occurrence of energy transfer between lanthanide(III) ions and d-block ions in dinuclear complexes where the metal complex fragments are well separated and connected only by hydrogen bonds between their respective ligands suggests a Förster mechanism.[36] It is worth pointing out that the situation regarding d → f energy transfer is further confused by a variety of other factors. The selection rules alluded to above are not absolute but may be circumvented by the involvement of 4f−5d transitions;[34] thus, for example, the $^4I_{9/2}$ and $^4F_{9/2}$ levels

(30) Martinus, H.; Werts, V.; Ronald, Y.; Jukes, T. F.; Verhoeven, J. W. *Phys. Chem. Chem. Phys.* **2002**, *4*, 1542.
(31) Dexter, D. L. *J. Chem. Phys.* **1953**, *21*, 836.
(32) Förster, T. *Discuss. Faraday Soc.* **1959**, *27*, 7.
(33) Sato, S.; Wada, M. *Bull. Chem. Soc. Jpn.* **1970**, *43*, 1955.
(34) de Sá, G. F.; Malta, O. L.; de Mello Donegá, C.; Simas, A. M.; Longo, R. L.; Santa-Cruz, P. A.; da Silva, E. F. *Coord. Chem. Rev.* **2000**, *196*, 165.
(35) Gonçalves e Silva, F. R.; Malta, O. L.; Reinhard, C.; Güdel, H.-U.; Piguet, C.; Moser, J. E.; Bünzli, J.-C. G. *J. Phys. Chem.* **2002**, *106*, 1670.
(36) Brayshaw, P. A.; Bünzli, J.-C. G.; Froidevaux, P.; Harrowfield, J. M.; Kim, Y.; Sobolev, A. N. *Inorg. Chem.* **1995**, *34*, 2069.

of Er(III) may play a role in acting as energy acceptors despite having $|\Delta J| = 3$ with respect to the ground state. For Yb(III), an alternative energy-transfer mechanism has been suggested by Horrocks and co-workers;[37] this involves a two-step forward-and-back electron-transfer process and relies on the fact that Yb(III) may be transiently reduced to Yb(II) if the sensitizer is a good electron donor in its excited state. Güdel and co-workers suggested that "phonon-assisted" energy transfer could occur from the ligand to Yb(III) in $[Yb(dipic)_3]^{3-}$, where there is zero spectral overlap between the phosphorescence of dipicolinate and the f−f absorption of Yb(III); in this case, the excess energy is dissipated as vibrations of the strongly mechanically coupled chromophore−quencher system.[38] This is a possibility in Re−Yb, in which the two metal ions share a common bridging ligand.

Conclusions

The luminescent mononuclear d-block complexes $[Re(bpym)(CO)_3Cl]$ and $(bpym)PtCF_3$, which contain 2,2′-bipyrimidine as a ligand, act as "complex ligands", allowing the formation of d−f heterodinuclear complexes by the addition of a $Ln(diketonate)_3$ unit at the second diimine site. In the resulting series of compounds Re−Ln and Pt−Ln, where Ln is a NIR-luminescent lanthanide complex of Yb(III), Nd(III), or Er(III), excitation of the MLCT absorption of the d-block chromophore results in fast Re → Ln or Pt → Ln energy transfer with concomitant sensitized luminescence from the lanthanide unit. In the dinuclear complexes, the characteristic ^{3}MLCT luminescence of the d-block chromophore is completely quenched in each case in the solid state.

Experimental Section

General Details. The following materials were prepared according to published procedures: $[Re(bpym)(CO)_3Cl]$,[20] $[Pt(bpym)Cl_2]$,[22] $[Nd(hfac)_3(H_2O)_2]$, and $[Gd(hfac)_3(H_2O)_2]$.[39] The reagents $[Yb(fod)_3(H_2O)_2]$, α,α,α-trifluoro-4-ethynyl-toluene, 2,2′-bipyrimidine, K_2PtCl_4, and $Re(CO)_5Cl$ were purchased from Aldrich and used as received. ^{1}H NMR spectra were recorded on a JEOL GX-400 instrument at 400 MHz, IR spectra were recorded on a Perkin-Elmer Spectrum One spectrophotometer, and luminescence titrations were measured on a Perkin-Elmer LS-50 fluorimeter.

Photophysical Studies. Solution spectroscopic investigations were carried out in dichloromethane (Carlo Erba, spectrofluorimetric grade) using 1-cm-path-length cuvettes. Absorption spectra were recorded with a Perkin-Elmer λ40 spectrophotometer. Uncorrected emission spectra were obtained with an Edinburgh FLS920 spectrometer (continuous 450 W Xe lamp) equipped with a peltier-cooled Hamamatsu R928 photomultiplier tube (185−900 nm) or with a Perkin-Elmer LS-50B spectrofluorimeter equipped with a Hamamatsu R3896 photomultiplier. Emission lifetimes of the Pt complexes in the visible region were obtained with an IBH time-correlated single-photon-counting spectrometer using a nano-LED at 455 nm as the excitation source; the time resolution of the instrument was 1 ns. Luminescence quantum yields were obtained from dilute samples (≈10^{-5} M) using the method of Demas and Crosby,[40] employing $[Ru(bipy)_3][PF_6]_2$ in air-equilibrated water as the standard ($\phi = 0.028$).[41]

The steady-state NIR luminescence spectra were obtained with an Edinburgh FLS920 spectrometer equipped with a Hamamatsu R5509-72 supercooled photomultiplier tube at 193 K and a TM300 emission monochromator with NIR grating blazed at 1000 nm. An Edinburgh Xe900 450 W xenon arc lamp was used as the excitation light source. Corrected spectra were obtained via a calibration curve supplied with the instrument. The NIR emission lifetimes were obtained by using the third harmonic (355 nm) of a Nd:YAG laser (JK Lasers) with a 20 ns pulse and 1−2 mJ of energy per pulse as the source. The detector was a liquid-nitrogen-cooled germanium and preamplifier (Northcoast Scientific Corp. model EO-817L). The solid-state luminescence lifetimes were obtained by spreading some sample in the powder state on a quartz support (25 × 25 mm).

Experimental uncertainties in the photophysical measurements are estimated to be ±8% for lifetime determinations, ±2 and ±5 nm for absorption and emission peaks, respectively, and ±20% for luminescence quantum yields.

Syntheses. (A) General Procedure for the Synthesis of Pt−Acetylide Complexes. $Pt(bpym)Cl_2$ (0.15 g, 0.35 mmol), anhydrous CuI (7 mg), and dry $^iPr_2NH$ (2 cm^3) were added to dry, degassed dichloromethane (30 cm^3) under N_2, and the mixture was stirred for 10 min, after which the appropriate acetylene (2.8 mmol, 8 equiv) was added. The resulting suspension was stirred under N_2 at room temperature and protected from light for 2−5 days. The reaction mixture could be sonicated to facilitate the reaction. By the end of reaction, the suspension had dissolved to give a yellow−deep-red solution that was evaporated to dryness. The solid residue was dried under vacuum, and the product was purified by column chromatography on alumina, eluting with CH_2Cl_2. The fraction containing the product was collected and reduced in volume to 5 cm^3. The complex was precipitated by the addition of hexane, filtered, washed with hexane and ether, and dried under vacuum. The complexes are air- and moisture-stable solids of an orange−red color that are soluble in CH_2Cl_2, acetone, and tetrahydrofuran and are insoluble in ether and hexane.

(1) Data for (bpym)PtH. Color: dark red. Yield: 73%. FAB−MS *m*/*z*: 578 (22%, $[M + Na]^+$), 555 (50%, M^+). Anal. Calcd for $C_{24}H_{16}N_4Pt$: C, 51.9; H, 2.9; N, 10.1. Found: C, 51.6; H, 2.6; N, 9.8. ^{1}H NMR (CD_2Cl_2): δ 9.96 (2H, dd, bpym H^4 or H^6), 9.27 (2H, dd, bpym H^6 or H^4), 7.77 (2H, t, bpym H^5), 7.47 (4H, d, phenyl H^2/H^6), 7.30 (4H, t, phenyl H^3/H^5), 7.20 (2H, m, phenyl H^4).

(2) Data for (bpym)PtMe. Color: red. Yield: 67%. FAB−MS *m*/*z*: 606 (24%, $[M + Na]^+$), 583 (60%, M^+). Anal. Calcd for $C_{26}H_{20}N_4Pt$: C, 53.5; H, 3.5; N, 9.6. Found: C, 54.0; H, 3.5; N, 9.3. ^{1}H NMR (CD_2Cl_2): δ 9.97 (2H, dd, bpym H^4 or H^6), 9.26 (2H, dd, bpym H^6 or H^4), 7.76 (2H, t, bpym H^5), 7.37 (4H, d, phenyl), 7.11 (4H, d, phenyl), 2.35 (6H, s, Me).

(3) Data for $(bpym)PtCF_3$. Color: orange. Yield: 80%. FAB−MS *m*/*z*: 714 (4%, $[M + Na]^+$), 691 (14%, M^+). Anal. Calcd for $C_{26}H_{14}F_6N_4Pt$: C, 45.2; H, 2.0; N, 8.1. Found: C, 44.8; H, 1.8; N, 8.1. ^{1}H NMR (CD_2Cl_2): δ 9.88 (2H, dd, bpym H^4 or H^6), 9.30 (2H, dd, bpym H^6 or H^4), 7.79 (2H, t, bpym H^5), 7.56 (8H, m, phenyl).

(B) Synthesis of Heterodinuclear Pt(II)−Ln(III) Complexes Pt−Nd and Pt−Gd. These complexes were obtained by slow (3−5

(37) Horrocks, W. D.; Bolender, J. P.; Smith, W. D.; Supkowski, R. M. *J. Am. Chem. Soc.* **1997**, *119*, 5972.
(38) Reinhard, C.; Güdel, H. U. *Inorg. Chem.* **2002**, *41*, 1048.
(39) Hasegawa, Y.; Kimura, Y.; Murakoshi, K.; Wada, Y.; Kim, J.; Nakashima, N.; Yamanaka, T.; Yanagida, S. *J. Phys. Chem.* **1996**, *100*, 10201.
(40) Demas, J. N.; Crosby, G. A. *J. Phys. Chem.* **1971**, *75*, 991.
(41) Nakamuru, K. *Bull. Chem. Soc. Jpn.* **1982**, *55*, 2697.

Table 8. Crystal, Data Collection, and Refinement Details for Crystal Structures[a]

complex	(bpym)PtH	(bpym)PtCF$_3$	Re−Yb	Pt−Gd·(C$_6$H$_6$)	Pt−Nd·(C$_6$H$_6$)
formula	$C_{24}H_{16}N_4Pt$	$C_{26}H_{14}F_6N_4Pt$	$C_{41}H_{36}ClF_{21}N_4O_9ReYb$	$C_{47}H_{23}F_{24}GdN_4O_7Pt$	$C_{47}H_{23}F_{24}N_4NdO_7Pt$
mol wt	555.5	691.5	1522.4	1564.0	1551.0
cryst syst	orthorhombic	monoclinic	triclinic	monoclinic	triclinic
space group	*Pbcn*	*C*2/*c*	$P\bar{1}$	*P*2(1)/*c*	$P\bar{1}$
a, Å	17.316(3)	29.101(4)	11.791(4)	19.9826(17)	11.325(3)
b, Å	10.919(2)	7.3072(9)	12.177(3)	11.2877(12)	20.578(3)
c, Å	10.0939(19)	28.224(4)	18.722(4)	25.436(3)	23.106(4)
α, deg	90	90	81.78(2)	90	90.358(12)
β, deg	90	120.644(11)	88.31(2)	109.142(6)	95.917(12)
γ, deg	90	90	82.889(17)	90	103.55(2)
V, Å^3	1908.5(6)	5163.6(12)	2639.7(13)	5420.1(9)	5204.3(16)
Z	4	8	2	4	4
ρ, g cm^{-3}	1.933	1.779	1.915	1.917	1.980
cryst size, mm^3	0.5 × 0.2 × 0.2	0.5 × 0.15 × 0.15	0.3 × 0.1 × 0.1	0.5 × 0.3 × 0.1	0.5 × 0.3 × 0.15
μ, mm^{-1}	7.370	5.499	4.230	3.926	3.812
data, restraints, params	2192, 0, 132	5883, 0, 319	12024, 0, 712	12397, 0, 674	23673, 0, 1454
final R1, wR2[b]	0.0184, 0.0445	0.0407, 0.1191	0.0598, 0.1609	0.0536, 0.1541	0.0684, 0.1661

[a] All data sets were collected on a Bruker SMART diffractometer with Mo Kα radiation (λ = 0.710 73 Å, 2θ limit = 55°) at 173 K. [b] The value of R1 is based on selected data with $F > 4\sigma(F)$; the value of wR2 is based on all data.

days) partial evaporation of a mixed benzene/heptane solution (4:1, v/v; initial volume approximately 10 cm^3) containing (bpym)PtCF$_3$ and Ln(hfac)$_3$·2H$_2$O (Ln = Nd or Gd) in a 1:1 molar ratio (ca. 50 μmol of each). The dark-red crystals of the heterodinuclear complex that formed were filtered off, washed with hexane, and vacuum-dried at room temperature. The complexes are air- and moisture-stable solids of a dark-red color. Attempts at a similar synthesis using heavier lanthanides (Ln = Er or Yb) gave only crystals of the starting materials.

(1) Data for Pt−Nd. Yield: 64%. Anal. Calcd for $C_{41}H_{17}F_{24}N_4NdO_6Pt$: C, 33.8; H, 1.2; N, 3.9. Found: C, 34.2; H, 1.4; N, 3.7.

(2) Data for Pt−Gd (as Benzene Solvate). Yield: 65%. Anal. Calcd for $C_{47}H_{23}F_{24}N_4GdO_6Pt$: C, 36.1; H, 1.5; N, 3.6. Found: C, 36.0; H, 1.6; N, 3.7.

(C) Synthesis of Heterodinuclear Re(I)−Yb(III) Complex Re−Yb. [Re(CO)$_3$Cl(bpym)] (0.030 g, 65 μmol) and Yb(fod)$_3$(H$_2$O)$_2$ (0.073 g, 65 μmol) were dissolved in CH$_2$Cl$_2$ (15 cm^3), and the red solution was stirred for 10 min. Hexane (15 cm^3) was added to the solution. Concentration of the solution resulted in the precipitation of the orange−red dinuclear complex Re−Yb, which was filtered, washed with a small amount of hexane, and vacuum-dried. The complex is an air-stable orange solid, obtained in 67% yield; it is soluble in benzene, CH$_2$Cl$_2$, and acetone and insoluble in hexane. Large needlelike crystals suitable for X-ray analysis were readily formed by slow evaporation of a mixed CH$_2$Cl$_2$/hexane solution of the complex. Anal. Calcd for $C_{41}H_{36}ClN_4O_9ReYbF_{21}$: C, 32.4; H, 2.4; N, 3.7. Found: C, 33.0; H, 2.1; N, 3.8. IR (CH$_2$Cl$_2$): 2033, 1936, 1915 cm^{-1}.

The analogous complexes Re−Nd and Re−Er were prepared in the same way.

(1) Data for Re−Er. Yield: 77%. Anal. Calcd for $C_{41}H_{36}ClN_4O_9ReErF_{21}$: C, 32.5; H, 2.4; N, 3.7. Found: C, 32.4; H, 2.1; N, 3.9. IR (CH$_2$Cl$_2$): 2033, 1936, 1915 cm^{-1}.

(2) Data for Re−Nd. Yield: 71%. Anal. Calcd for $C_{41}H_{36}ClN_4O_9ReNdF_{21}$: C, 33.0; H, 2.4; N, 3.7. Found: C, 32.6; H, 2.2; N, 3.8. IR (CH$_2$Cl$_2$): 2032, 1935, 1914 cm^{-1}.

X-ray Crystallography. Suitable crystals were mounted on a Bruker SMART-CCD diffractometer equipped with graphite-monochromatized Mo Kα radiation. Crystallographic measurements were carried out at 173 K; details of the crystal, data collection, and refinement parameters are summarized in Table 8, and selected structural parameters are collected in Tables 1, 2, and 4−6. After integration of the raw data and merging of equivalent reflections, an empirical absorption correction was applied based on comparison of multiple symmetry-equivalent measurements.[42] The structures were solved by direct methods and refined by full-matrix least squares on weighted F^2 values for all reflections using the SHELX suite of programs.[43]

The structural determinations of (bpym)PtH and (bpym)PtCF$_3$ were straightforward. The structural determinations of the dinuclear complexes were complicated by disorder involving the F atoms associated with the CF$_2$CF$_2$CF$_3$ chains in Re−Yb and by rotational disorder of the CF$_3$ groups of the hfac ligands in Pt−Nd and Pt−Gd. In Pt−Gd, the F atoms of three of the CF$_3$ groups [involving F(91)−F(93), F(31)−F(33), and F(71)−F(73)] could be refined in two alternate positions with approximately 50:50 site occupancy in each. In the other cases, the disorder could not be resolved, and the F atoms accordingly have rather high thermal parameters; the highest residual electron density peaks are close to these F atoms. To keep the refinements stable, some of these F atoms and their associated C atoms were refined with isotropic thermal parameters. These problems are typical of complexes of this type containing peripheral fluorocarbon chains.[18]

Acknowledgment. We thank the Royal Society, London, U.K. (postdoctoral fellowship to N.M.S.), and EPSRC, Swindon, U.K. (Ph.D studentship to T.L. and postdoctoral fellowship to Z.R.B.), for financial support. We thank Dr. G. Di Marco as a proponent of Dr. G. Calogero's research activity program, entitled "Synthesis and Study of Luminescent Compounds Based on Transition-Metal Complexes for Sensor Applications" and supported by the CNR short-term mobility program, 2003.

Supporting Information Available: CIF file containing data for the five crystal structures Re−Yb, Re−Nd, Re−Er, Pt−Nd, and Pt−Gd. This material is available free of charge via the Internet at http://pubs.acs.org.

IC048875S

(42) Sheldrick, G. M. *SADABS*: *A Program for Absorption Correction with the Siemens SMART System*; University of Gottingen: Gottingen, Germany, 1996.

(43) *SHELXTL Program System*, version 5.1; Bruker Analytical X-ray Instruments Inc.: Madison, WI, 1998.